All-optical mode switching with a graphene-buried polymer waveguide directional coupler

JIANG, Lianzhong; CHIANG, Kin Seng

Published in:
Optics Letters

Published: 15/05/2022

Document Version:
Post-print, also known as Accepted Author Manuscript, Peer-reviewed or Author Final version

Published version (DOI):
10.1364/OL.458204

Publication details:
JIANG, L., & CHIANG, K. S. (2022). All-optical mode switching with a graphene-buried polymer waveguide directional coupler. *Optics Letters*, *47*(10), 2414-2417. Advance online publication. https://doi.org/10.1364/OL.458204

All-optical mode switching with a graphene-buried polymer waveguide directional coupler

LIANZHONG JIANG AND KIN SENG CHIANG*

Department of Electrical Engineering, City University of Hong Kong, 83 Tat Chee Avenue, Kowloon, Hong Kong SAR, China
**Corresponding author: eeksc@cityu.edu.hk*

Received XX Month XXXX; revised XX Month, XXXX; accepted XX Month XXXX; posted XX Month XXXX (Doc. ID XXXXX); published XX Month XXXX

We demonstrate all-optical mode switching with a graphene-buried polymer waveguide asymmetric directional coupler by using the photothermal effect of graphene, where TE-polarized pump light and TM-polarized signal light are employed to maximize pump absorption and minimize graphene-induced signal loss. Our experimental device, which uses a graphene length of 6.2 mm, shows a pump absorption of 3.4 dB (at 980 nm) and a graphene-induced signal loss of 0.1 dB. The device can spatially switch between the fundamental mode and the higher-order mode with extinction ratios larger than 10 dB (at 1580 nm) and switching times slightly shorter than 1 ms at a pump power of 36.6 mW. Graphene-buried polymer waveguides offer many new possibilities for the realization of low-power all-optical control devices.

http://dx.doi.org/10.1364/OL.99.099999

All-optical control devices have attracted much attention for their important applications in all-optical signal processing [1]. To realize efficient all-optical control functions, optical media with strong nonlinearities are required. In recent years, the availability of graphene as a nonlinear optical medium [2,3] has opened up new opportunities for the development of all-optical control devices. In particular, graphene's photothermal effect, which converts absorbed light into heat, has been explored for the construction of all-optical switches on fiber [4–6] and waveguide platforms [7–9].

Recently we have demonstrated an all-optical switch with a switching power as low as 6 mW by using graphene's photothermal effect in a graphene-buried Mach-Zehnder interferometer formed with polymer waveguides [9]. The graphene-buried polymer waveguide platform offers a number of distinct advantages. First, it is known that a graphene film can strongly absorb the light wave with a polarization in parallel with the graphene surface and does not absorb the light wave with a polarization perpendicular to the graphene surface [10,11]. Being a low-index-contrast waveguide, a graphene-buried polymer waveguide supports almost pure linearly polarized modes, which allows the use of TE-polarized pump (whose electric field is mainly parallel to the graphene surface) and TM-polarized signal (whose electric field is mainly perpendicular to the graphene surface) to optimize pump absorption without inducing significant signal loss [9] (the small parallel electric-field component of the TM-polarized signal cause only weak absorption). This property is not available with high-index-contrast waveguides that support hybrid modes, which have comparable parallel and perpendicular electric-field components. Second, the spin-coating process available for the fabrication of polymer waveguides allows a graphene film to be placed inside or close to the waveguide core [9–11] to facilitate pump absorption and heat transfer. Third, the large thermo-optic coefficient of polymer material can provide a large refractive-index change from the heat generated by graphene. In this Letter, we demonstrate all-optical switching between two spatial modes with a graphene-buried polymer waveguide asymmetric directional coupler (DC). This new all-optical control function could find applications in mode multiplexing systems.

Nonlinear symmetric DCs formed with two parallel identical single-mode waveguides for all-optical switching based on the Kerr effect have been studied for many years (see, for example, [12,13]). Because of the lack of material with strong third-order nonlinearity, the switching powers required are high and can only be delivered with short-pulse lasers. For example, a nonlinear DC fabricated with AlGaAs waveguides requires a switching power of 42 W [12]. Here we propose a DC formed with a single-mode waveguide and a few-mode waveguide for achieving all-optical mode switching. Our experimental device is fabricated with polymer waveguides with graphene buried in the single-mode waveguide. With graphene's large photothermal effect and the use of orthogonal polarizations for the pump (at 980 nm) and the signal light, we achieve a switching power of 36.6 mW at extinction ratios larger than 10 dB (for a signal wavelength of 1580 nm). The actual pump power absorbed by graphene is 7.7 mW. The switching times are slightly shorter than 1 ms.

Figure 1(a) shows the structure of the proposed all-optical mode switch, which is an asymmetric DC formed with a graphene-buried single-mode waveguide (Core 1) and a few-mode waveguide (Core 2). Both the pump and the signal light are launched into Core 1. The pump and the signal wavelength are chosen to be 980 nm and 1550 nm, respectively. For the buried graphene film to effectively absorb the pump light without inducing significant loss to the signal light, the pump and the signal light are set to be TE-polarized and TM-

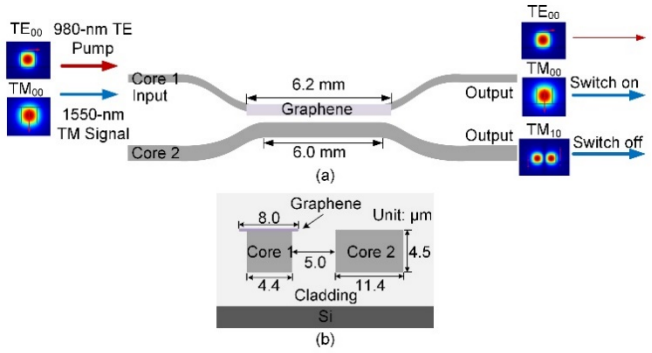

Fig. 1. Schematic diagrams showing (a) the proposed graphene-buried polymer waveguide asymmetric DC for all-optical mode switching and (b) the cross section of the DC.

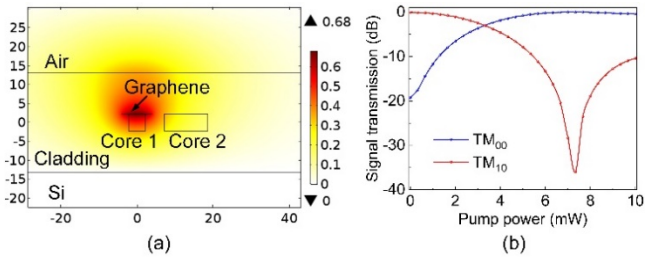

Fig. 2. (a) Temperature distribution of the graphene-buried DC calculated for a pump power of 1.0 mW and (b) variations of the transmission characteristics of the DC with the pump power for the TM_{00} mode of Core 1 and the TM_{10} mode of Core 2.

polarized, respectively [9–11]. The DC is designed to function as a mode (de)multiplexer when the pump is turned off, i.e., the switch is off. For the DC to function as a mode (de)multiplexer, the phase-matching condition between the two cores at the signal wavelength must be satisfied, i.e., the effective index of the fundamental mode (the TM_{00} mode) of Core 1 is equal to that of the higher-order mode (the TM_{10} mode) of Core 2. In that case, the signal light launched into the TM_{00} mode of Core 1 can be transferred completely to the TM_{10} mode of Core 2 with a suitable coupler length [14]. As the pump light has a tight mode confinement and no phase matching is available at the pump wavelength, the pump light passes through Core 1 without coupling to Core 2 and is absorbed by the graphene film in Core 1. The pump light absorbed by graphene is converted into heat, which raises the temperatures of the two cores. As the temperature rise in Core 1 is larger than that in Core 2, the thermo-optically induced refractive-index change in Core 1 is larger than that in Core 2. As a result, the phase-matching condition at the signal wavelength is upset and the coupling between the two cores is weakened. At a high enough pump power, the coupling between the two cores can become negligible, in which case the switch is considered to be turned on. In other words, the mode coupling effect of the DC can be deactivated by the pump light, which leads to a switching between the TM_{00} mode of Core 1 and the TM_{10} mode of Core 2 at the signal wavelength. The device works equally well with the signal light launched into the TM_{10} mode of Core 2.

In our study, we use the polymer materials EpoCore and EpoClad (Micro Resist Technology) as the core and the cladding material of the waveguides, respectively [9–11,14,15], whose refractive indices measured at 1530 nm are 1.575 and 1.560, respectively. We employ a mode solver (COMSOL) to calculate the effective indices and the fields of the modes and a 3D finite-difference beam propagation method (BPM) (3DFD-BPM, RSoft) to tune the waveguide parameters to optimize the performance of the DC. In our final design, the height of the two cores is 4.5 μm and the widths of Core 1 and Core 2 are 4.4 μm and 11.4 μm, respectively. Core 2 supports four spatial modes with two polarizations. The gap between the two cores is 5.0 μm. The length of the parallel section of the cores is 6.0 mm. The graphene film, which is placed symmetrically on the surface of Core 1, has a width of 8.0 μm and a length of 6.2 mm, which covers a small part of the S-bends connected to the two ends of the DC. The device is formed on a silicon (Si) substrate. Figure 1(b) shows a schematic diagram of the cross section of the DC together with the core dimensions.

To calculate the switching characteristics of the DC, we treat the DC as a thermo-optic switch driven by the pump power absorbed by graphene. We first calculate the graphene-induced losses by applying the interface model of graphene, whose complex conductivities are $6.0840 \times 10^{-5} - 1.5959 \times 10^{-6}i$ and $6.0792 \times 10^{-5} - 8.6160 \times 10^{-6}i$ for 980 nm and 1550 nm, respectively [10]. For a 6.2-mm length of graphene, the absorption for the TE-polarized pump light is 18.9 dB or 98.7%, while that for the TM-polarized signal light is 0.4 dB or 9%. We assume that all the pump light absorbed is converted into heat and the very high thermal conductivity of graphene (~5000 W/m·K [16]) allows the heat to be distributed quickly and evenly on the graphene film. We then model graphene as a sheet of uniform heat source with zero thickness and calculate the temperature distribution with the heat transfer module in COMSOL [5,9], where the thermal conductivities of the polymer material and silicon are set at 0.12 W/m·K and 130 W/m·K, respectively. As shown by the calculation results in Fig. 2(a), for a 1-mW pump power, the average temperature of Core 1 is increased by ~0.5 K and that of Core 2 by ~0.2 K. We next calculate the refractive-index distribution from the temperature distribution by assuming a thermo-optic coefficient of -1.0×10^{-4} for the polymer material. With the knowledge of the refractive-index distribution at a given pump power, we calculate the normalized output signal powers with the BPM. The transmission characteristics of the switch calculated at different pump powers are shown in Fig. 2(b). The pump power required for achieving mode switching with a maximum extinction ratio is 7.3 mW, which is significantly lower than the electric powers required in conventional electrically driven thermo-optic polymer waveguide mode switches that employ metal electrode heaters with buffer layers [14], thanks to the direct placement of the graphene film on the core.

We fabricated the device with our in-house microfabrication process [9–11,14,15]. First, an 11.0 μm EpoClad film was spin-coated on a silicon substrate as the lower cladding. An EpoCore film with a thickness slightly larger than 4.5 μm was next spin-coated onto the lower cladding and patterned by photolithography and wet-etching. An EpoClad film with a thickness slightly larger than the core layer was spin-coated onto the sample as the mid-cladding and then etched down to the cores by reactive ion etching (RIE) to form a flat surface for graphene transfer. The RIE process also allowed the thickness of the core layer to be trimmed to the desired value. A commercial monolayer graphene film grown on a copper foil (Hefei Vigon Material Technology) with a polymethyl-methacrylate (PMMA) buffer was wet-transferred onto the sample, and the PMMA buffer was removed by acetone. The sample actually

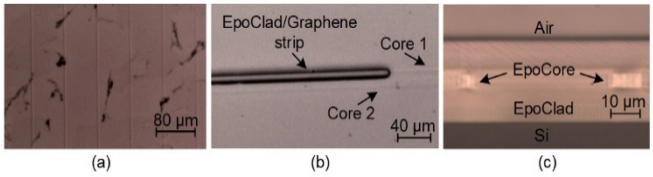

Fig. 3. Microscopic images showing (a) the sample after graphene transfer, (b) an etched EpoClad/graphene strip on Core 1, and (c) the cross sections of Core 1 and Core 2.

consisted of a large number of waveguides. Figure 3(a) shows a top view of the sample after graphene transfer, where graphene and PMMA residues can be seen. As shown in Fig. 3(a), there exist some cracks and holes on the graphene film, which were caused by the transfer process. The graphene film was next patterned and etched into strips of the desired size with an EpoClad mask and the O_2 plasma etching process. Figure 3(b) shows an etched EpoClad/graphene strip on Core 1. Finally, a 10.0 μm EpoClad film was spin-coated onto the sample as the upper cladding. The total length of the fabricated device was ~12 mm. Figure 3(c) shows microscopic images of the cross sections of Core 1 and Core 2 taken from an end face of the device.

To characterize the fabricated device, we launched TE-polarized pump light into Core 1. To demonstrate mode switching, we could launch TM-polarized signal light either into Core 1 as the TM_{00} mode or into Core 2 as the TM_{10} mode. As it was difficult to excite the TM_{10} mode of Core 2 to a high purity, we chose to launch both the pump and the signal light into Core 1 with a 980/1550 wavelength-division multiplexer and a lensed fiber. The pump and the signal light were generated from a 980 nm laser diode (Lumentum, S27-7402-360-AL) and a tunable laser (Keysight), respectively, and individual fiber polarization controllers were used to control their polarization states. The output powers were monitored with a power meter (Newport 1830-C) and the output near-field images were taken with an infrared camera (Hamamatsu, C2714).

We first turned off the pump and measured the coupling efficiency of the DC for different signal wavelengths. Here the coupling efficiency is defined as the output power of the TM_{10} mode from Core 2 normalized to the total output power from both cores. As shown in Fig. 4(a), the coupling efficiency at 1550 nm is 76% and the highest value achieved is 92% at 1580 nm. The deviations from the simulation results are likely caused by the fabrication errors in the control of the waveguide parameters. We next took the output near-field images from both cores by turning on only the pump or the signal. As shown in Figs. 4(b) and (c), the pump light always stays in Core 1 mainly as the fundamental mode. On the other hand, as shown in Figs. 4(d) and (e), most of the signal light (at 1580 nm) couples to the higher-order mode of Core 2. For both the pump and the signal wavelength, the output power for the TE polarization is much weaker than that of the TM polarization. These results confirm that the DC indeed operates as a mode (de)multiplexer for the signal wavelength and the graphene film attenuates TE-polarized light much more than TM-polarized light. By comparing the output powers of the TE and the TM polarization, we estimated that the absorption for the TE-polarized pump was ~3.4 dB or ~55%. We also measured the absorption losses of the pump light with a number of straight reference graphene-buried single-mode waveguides formed on the same sample, and found that the absorption losses varied from 3.1 dB to 4.0 dB, which is consistent

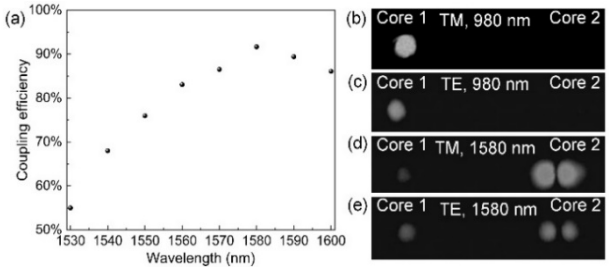

Fig. 4. (a) Variation of the coupling efficiency with the signal wavelength measured with the pump turned off, and output near-field images for (b) TM-polarized light at 980 nm, (c) TE-polarized light at 980 nm, (d) TM-polarized light at 1580 nm, and (e) TE-polarized light at 1580 nm.

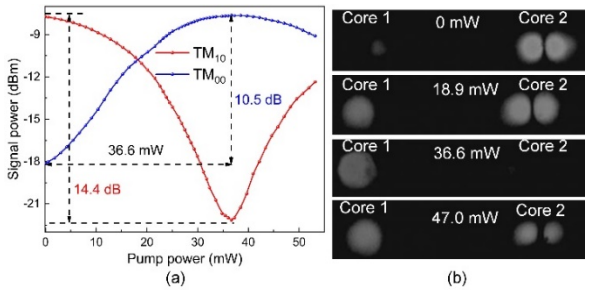

Fig. 5. (a) Variations of the output signal powers of the TM_{00} mode from Core 1 and the TM_{10} mode from Core 2 with the input pump power for the signal wavelength 1580 nm, and (b) output near-field images for the signal light taken at different pump powers.

with the measurement result for the DC. To measure the graphene-induced signal loss, we compared the output power of the TM-polarized signal light from the device with that from a reference DC without graphene, and found that the graphene-induced signal loss was of the order of 0.1 dB. Both the pump and the signal absorption measured for the experimental device are smaller than the simulation values, which, we believe, is caused by the presence of cracks and holes on the graphene film, as shown in Fig. 3(a), as the presence of such defects reduces the useful length of the graphene film for light absorption and hence increases the input pump power required for the generation of the same amount of heat.

We next measured the switching characteristics of the device by turning on both the pump and the signal light and varying the pump power, where the pump light was set to be TE-polarized and the signal light TM-polarized. The input signal power measured from the lensed fiber was fixed at 0.7 mW. We placed a band-pass filter at the output end of the device to filter out the residue pump light. The output signal powers (at 1580 nm) of the TM_{00} mode from Core 1 and the TM_{10} mode from Core 2, measured at different input pump powers, are shown in Fig. 5(a). As the input pump power increases, the output power of the TM_{10} mode from Core 2 decreases, while that of the TM_{00} mode from Core 1 increases. When the input pump reaches a maximum value of 14.4 dB, and that of the TM_{00} mode reaches 10.5 dB. The output near-field images taken at different pump powers, as shown in Fig. 5(b), confirm switching between the two modes. The measured switching characteristics agree qualitatively with the simulation results shown in Fig. 2(b). The

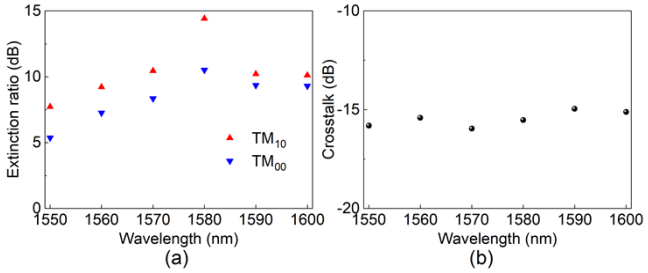

Fig. 6. (a) Extinction ratios and (b) modal crosstalk measured at different signal wavelengths.

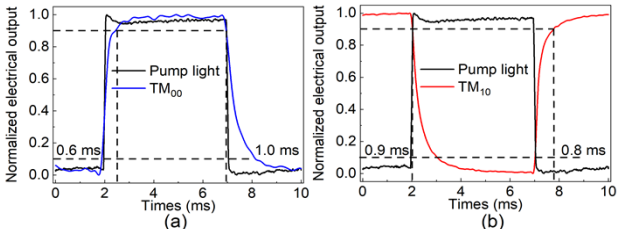

Fig. 7. Switching times measured for (a) the TM_{00} mode from Core 1 and (b) the TM_{10} mode from Core 2 at the signal wavelength 1580 nm.

measured extinction ratios are lower, which can be attributed to the lower coupling efficiency of the fabricated DC, compared with the ideal DC used in the simulation. The switching power shown in Fig. 5(a) is the input pump power measured from the lensed fiber. With the fiber-waveguide coupling loss (~1.4 dB) and the propagation loss (~2.0 dB/cm) excluded, the actual switching power is much smaller. To directly measure the actual pump power absorbed by graphene, we compared the output pump powers for the TE and the TM polarization at a fixed input pump power of 36.6 mW. The difference was 7.7 mW, which can be regarded as the actual amount of the pump power converted into heat for achieving all-optical mode switching. Given the uncertainties in power measurements (about ±0.3 dB) and the parameters used in the theoretical model, the measurement result 7.7 mW agrees well with the simulation result 7.3 mW. By improving the fabrication process and the quality of the graphene film with an optimized transfer method [17], it should be possible to further increase the extinction ratios and reduce the switching power. Another way to operate the device is to switch between the TE and the TM polarization of the pump light with the pump power fixed at 36.6 mW.

The extinction ratios measured at different signal wavelengths are shown in Fig. 6(a). We also measured the modal crosstalk caused by the coupling between the TM_{00} mode of Core 2 and the TM_{00} mode of Core 1 by exciting the TM_{00} mode at Core 2 and measuring the output powers from the two cores. As shown in Fig. 6(b), the crosstalk is lower than –15 dB in the wavelength range from 1550 nm to 1600 nm. The insertion loss for the TM-polarized signal light measured at 1580 nm was 5.7 dB, which included 2.4 dB fiber-waveguide coupling loss at the input end. We also measured the coupling efficiencies of the device at different temperatures with a semiconductor heater placed at the bottom of the device. From 20 °C to 50 °C, the variations in the coupling efficiency at 1580 nm were within ±5%. The device shows a weak temperature sensitivity.

We finally measured the switching times of the device by modulating the pump laser between 0 mW and 36.6 mW with a 100-Hz square-wave electrical signal generated from a function generator (GW Instek, AFG-2225) and detecting the output signals with a photodetector and an oscilloscope (MCP Lab Electronic, DQ8304C). As shown by the waveforms in Fig. 7, the switching times are slightly shorter than 1.0 ms, which are comparable to those of electrically driven thermo-optic polymer waveguide mode switches [14,15]. We could further reduce the switching time by reducing the size of the device by using a smaller core separation.

In summary, we have demonstrated all-optical mode switching with a graphene-buried polymer waveguide asymmetric DC based on graphene's photothermal effect. Our experimental device can spatially switch between the TM_{00} mode of a single-mode core and the TM_{10} mode of a few-mode core with extinction ratios larger than 10 dB at a pump power of 36.6 mW with negligible graphene-induced signal loss. The switching times are slightly shorter than 1.0 ms. Our device can operate with continuous-wave lasers, which is necessary for applications like optical circuit switching. It is possible to cascade more similar DCs to achieve all-optical switching of more modes. Being a highly efficient platform for converting light into heat, a graphene-buried polymer waveguide can relax the pump power requirement and make possible the development of all-optical control functions that were not perceived before.

Funding. City University of Hong Kong (7005224).

Disclosures. The authors declare no conflicts of interest.

Data availability. Data underlying the results presented in this paper are not publicly available at this time but may be obtained from the authors upon reasonable request.

References

1. A. E. Willner, S. Khaleghi, M. R. Chitgarha, and O. F. Yilmaz, J. Lightw. Technol. **32**, 660 (2014).
2. H. Chen, C. Wang, H. Ouyang, Y. Song, and T. Jiang, Nanophotonics **9**, 2107 (2020).
3. C. Zhong, J. Li, and H. Lin, Front. Optoelectron. **13**, 114 (2020).
4. X. Gan, C. Zhao, Y. Wang, D. Mao, L. Fang, L. Han, and J. Zhao, Optica **2**, 468 (2015).
5. T. Hao, Z. Chang, and K. S. Chiang, Opt. Express **27**, 4216 (2019).
6. R. Chu, C. Guan, Y. Bo, J. Liu, J. Shi, J. Yang, P. Ye, P. Li, J. Yang, and L. Yuan, Opt. Lett. **45**, 177 (2020).
7. C. Qiu, C. Zhang, H. Zeng, and T. Guo, J. Lightw. Technol. **39**, 2099 (2021).
8. T. Guo, S. Gao, H. Zeng, L. Tang, and C. Qiu, J. Lightw. Technol. **39**, 4710 (2021).
9. L. Jiang, Q. Huang, and K. S. Chiang, Opt. Express **30**, 6786 (2022).
10. Z. Chang and K. S. Chiang, Opt. Lett. **41**, 2129 (2016).
11. Z. Chang and K. S. Chiang, Opt. Lett. **42**, 3868 (2017).
12. A. Villeneuve, J. S. Aitchison, B. Vögele, R. Tapella, J. U. Kang, C. Trevino, and G. I. Stegeman, Electron. Lett. **31**, 549 (1995).
13. J. S. Aitchison, A. Villeneuve, and G. I. Stegeman, Opt. Lett. **20**, 698 (1995).
14. Q. Huang, K. S. Chiang, and W. Jin, IEEE Photon. J. **10**, 6602714 (2018).
15. X. Wang, W. Jin, Z. Chang, and K. S. Chiang, Opt. Lett. **44**, 1480 (2019).
16. A. A. Balandin, S. Ghosh, W. Bao, I. Calizo, D. Teweldebrhan, F. Miao, and C. N. Lau, Nano Lett. **8**, 902 (2008).
17. H. Park, C. Lim, C. J. Lee, J. Kang, J. Kim, M. Choi, and H. Park, Nanotechnology **29**, 415303 (2018).